Kelvin Probe Force Microscope Observation of Chlorine-adsorbed TiO_2(110) Surfaces

Kumiko Hiehata[1], Akira Sasahara[1,2,3*], and Hiroshi Onishi[1]

[1]Department of Chemistry, Faculty of Science, Kobe University, Kobe 657-8501, Japan

[2]Japan Science and Technology Agency, Kawaguchi, Saitama 332-0012, Japan

*E-mail address: sasahara@jaist.ac.jp

The rutile titanium dioxide (TiO_2) (110) surface exposed to Cl_2 gas was examined using scanning probe microscopes. The Cl adatoms formed by Cl_2 dissociation were observed as bright spots in empty-state scanning tunneling microscope images. While 94% of the Cl adatoms were on the top of surface Ti atoms, the remaining 6% of the adatoms missed the on-top site. The Kelvin probe force microscope measurements revealed a local work function increase on the Cl adatoms. The electronegative Cl adatoms were proposed to accumulate electrons from the surface. The resultant dipole moments were directed from the vacuum to the surface, and hence the work function of the adatoms locally increased.

KEYWORDS: Kelvin probe force microscope, Scanning tunneling microscope, titanium dioxide, chlorine, work function, dipole moment

[3]Present address: School of Materials Science, Japan Advanced Institute of Science and Technology, Nomi 923-1292, Japan

1. Introduction

Chlorine additives influence the performance of heterogeneous catalysts where nanometer-sized metal particles are dispersed on a supporting material [1-3]. Selective dehydrogenation of cyclohexane ($C_6H_{12} \rightarrow C_6H_6+3H_2$) on an Al_2O_3-supported Ru catalyst was attributed to residual Cl from the $RhCl_3$ precursor [1]. 2-Butenal was reduced selectively to butanal ($CH_3CH=CHCHO+H_2 \rightarrow CH_3CH_2CH_2CHO$) on an Al_2O_3-supported Cu catalyst modified with either CCl_4 or CH_2Cl_2 [2]. The partial oxidation of ethene to ethylene oxide on an Al_2O_3-supported Ag catalyst was most effectively promoted by properly adding Cl additives to the catalyst [3]. The large electronegativity of Cl is thought to be the key for catalyst modification. The electron acceptability of an adsorbed Cl atom should be sensitive to the atomistic structure of the adsorption site, although the average extent of electron accumulation can be determined by X-ray photoelectron spectroscopy [4].

In the present study, the electron transfer of individual Cl adatoms was observed using a Kelvin probe force microscope (KPFM) [5]. The KPFM is based on the noncontact atomic force microscope (NC-AFM) [6], and provides the lateral distribution of the contact potential difference (CPD) between the probe and the sample. The lateral resolution of the CPD map reaches atomistic scales [7-10]. We have reported electron donation from individual Na adatoms [9], Pt adatoms [7], and nanometer-sized Pt clusters [11,12] to the titanium dioxide (TiO_2) substrate. The electron transfer from the surface to the Cl adatom should induce a dipole moment and hence an increase in the work function observable by KPFM.

Figure 1 shows the rutile TiO_2(110)-(1×1) surface employed as a substrate. The (1×1) surface consists of alternating rows of protruded O atoms and rows of fivefold-coordinated Ti atoms [13]. A Cl_2 molecule is dissociatively adsorbed on the (1×1) surface at room temperature, and the resultant two Cl adatoms are observed as bright spots on the Ti atom rows in empty-state scanning tunneling microscope (STM) images [14-16]. An ab-initio calculation showed that the on-top site of the fivefold-coordinated Ti atom is energetically favorable for the Cl adatom compared with the bridge site of the two Ti atoms [17].

2. Experimental Procedure

The experiments were performed using an ultrahigh-vacuum microscope (JEOL JSPM4500A) equipped with an Ar^+ sputtering gun (Thermo EX03) and low-energy electron diffraction optics (OCI BDL600). The base pressure was 2×10^{-8} Pa.

A TiO_2(110) wafer (Shinko-sha, $7\times1\times0.3$ mm^3) was supported on a Si wafer of the same size which was used as a resistive heater. The (1×1) surface was prepared by several cycles of Ar^+ sputtering and annealing at 1100 K. The sample temperature was monitored with an infrared pyrometer (Minolta TR630) through the transparent TiO_2 wafer, and therefore may be overestimated. Cl_2 was introduced to the vacuum chamber as a gas diluted with Ar (Tomoe-shokai, Cl_2 = 3%).

Imaging scans were carried out at room temperature. A conductive Si cantilever (MikroMasch NSC35) was used as a probe. The experimentally determined resonant frequency of the cantilevers was about 300 kHz. The KPFM and NC-AFM were operated in the constant frequency shift mode. The frequency and peak-to-peak amplitude of the modulation AC voltage for the KPFM measurements were 2 kHz and 2 V, respectively. In the NC-AFM measurement, the sample bias voltage was optimized so that the image with high contrast was obtained. The constant current STM images were acquired with a positive sample bias voltage using the Si cantilever as a probe.

3. Results and Discussion

The Cl_2-exposed TiO_2 surfaces prepared in our microscope were subjected to careful STM observation to identify surface species prior to KPFM imaging. Figure 2(a) shows an STM image of the sputter-annealed TiO_2(110) surface with the cross sections along the solid lines. The bright lines along the [001] direction represent the rows of fivefold-coordinated Ti atoms. The unoccupied states derived from the Ti 3d orbital contribute to electron tunneling [18]. Bright particles protruding from the Ti atom rows by 0.20 nm are reduced titanium oxide, TiO_x, inevitably formed upon the vacuum annealing. The number density of the TiO_x islands was about 0.01 nm^{-2}.

Figure 2 (b) shows an STM image of the TiO_2(110) surface exposed to the Ar-diluted Cl_2 gas for

200 L (1 L = 10^{-6} Torr s). Bright spots appeared with the number density of 0.41 nm^{-2}. The number density increased to 0.67 nm^{-2} on a 3,600 L exposed surface. We therefore assigned the spots to Cl adatoms. The Cl adatoms and the Ti-atom rows are represented by circles and solid lines in the illustration. The larger spots indicated by the arrows are the TiO_x islands.

Magnified images of the two regions in Fig. 2(b) are shown in Fig. 2(c) and 2(d). Ninety-four percent of the Cl adatoms were located on the Ti atom rows, and we labeled them A. Adatom A was higher than the Ti atom rows by 0.16±0.01 nm, as shown in the cross section (i), which is consistent to the previous report by Hebenstreit et al. [15] They found that the Cl adatoms on the Ti-atom rows protruded by 0.2 nm in empty state images. Less-bright spots were found between two adjacent Ti-atom rows and assigned to Cl atoms filling bridge O vacancies. We could not identify such spots, though our sputter-annealed surface exhibits 0.03 nm^{-2} of bridge O vacancies [19].

The remaining 6% of the Cl adatoms were shifted from the Ti atom rows. The shifted adatoms are presented as gray circles in Figs. 2(b)-2(d). One shifted adatom in Fig. 2(c) is labeled B. The cross section (ii) showed that the height of adatom B was 0.16 nm from the Ti atom rows. Some of adatoms B, which are surrounded by the dotted circles in the illustration in Fig. 2(b), were paired along the $[1\bar{1}0]$ direction. The height of the paired adatoms B reached 0.20 nm from the Ti atom rows, as shown in the cross section (iii). The paired adatoms may possibly be undissociated Cl_2 adsorbed on an O vacancy.

Figures 3(a) and 3(b) show the topography and work function map of the Cl_2-exposed surface, respectively. The contrast of the work function map (b) was adjusted so that the areas with a high work function are bright. Three different species, one major and two minor, are identified from the comparison of the topography and the work function. The major species are not recognized in the topography and are observed as bright spots with a uniform diameter of 1.0 nm in the work function image. One bright spot in the image in Fig. 3 is labeled (i). The cross sections of the topography and work function are shown in (1) of Fig. 3(c). The work function of species (i) was positively shifted relative to that of the surrounding TiO_2. The shifts are distributed from +0.05 to +0.12 eV, as shown in the histogram in Fig. 3(d) with an average of +0.08 eV. The number

density of species (i) was 0.32 nm^{-2}. Minor species labeled (ii) are observed as bright spots in the topography and also in the work function map. The topographic height of species (ii) is 0.10-0.16 nm. The cross section (2) in Fig. 3(c) passes the center of species (ii). The work function shift of species (ii) is distributed from +0.04 to +0.22 eV with an average of +0.11 eV. The number density of species (ii) was 0.01 nm^{-2}. The other minor species labeled (iii) protruded in the topography, and the work function was locally reduced. The height of species (iii) was around 0.15 nm, and the work function shifts ranged from -0.07 to -0.23 eV. The number density of species (iii) was 0.01 nm^{-2}.

We assign species (i) to Cl adatoms A. The electron accumulation by the adatom A forms a dipole moment directed from the vacuum to the surface, which locally increases the work function. The number density of the species (i), 0.32 nm^{-2}, was close to that of adatoms A in the STM images. The absence of the adatoms A in the topography suggests their limited topographic height. The identity of species (ii) remains unclear. Species (iii) were possibly the TiO_x islands. A negative shift of the work function has been reported on the TiO_x islands [20].

Consider the extent of electron accumulation on the major species (i), i.e., adatom A. In the parallel plate condenser model, electric dipole moments μ are distributed over the TiO_2 surface with number density σ. The work function shifts by $\Delta\phi = \sigma\mu/\varepsilon_0$. According to the results of an ultraviolet photoelectron spectroscopy study [14], the macroscopic work function of TiO_2(110) increased by 0.7 eV with Cl adatoms of 1.6×10^{18} atoms m^{-2}. The dipole moment per Cl adatom μ_{Cl} is thus 4×10^{-30} C m. This value is small compared with the moment induced by a Na adatom. When the TiO_2(110) surface was covered with a c(4×2) overlayer, the work function decreased by 3 eV [21]. The adatom density of the c(4×2) overlayer was later determined to be 1.3×10^{18} atoms m^{-2} [22]. The dipole moment per Na adatom μ_{Na} is 2×10^{-29} C m.

The local shift of the work function observed with KPFM was +0.08 eV for the Cl adatom and -0.35 eV for the Na adatom [9]. The ratio of absolute shifts, 8/35, agrees with $\mu_{Cl}/\mu_{Na} = 0.2$. This agreement suggests the applicability of KPFM in determining the quantity of electron transfer at solid surfaces with an atomistic resolution.

Finally, we consider the reason why adatoms A could not be recognized in the topography of Fig.

3(a). Figure 4(a) presents the constant frequency shift topography observed with a constant bias voltage. The bright lines extending to the [001] direction are the O-atom rows [23]. Brighter spots, which are assigned to the Cl adatoms A, appeared and increased in number with exposure to Cl_2-containing gas. In the illustration, the O-atom rows and Cl adatoms are presented by solid lines and circles, respectively. The number density of the adatoms was 0.40 nm^{-2}, which is consistent with that determined from the STM images, 0.41 nm^{-2}. Most of the Cl adatoms are at the middle of the two adjacent O-atom rows, as marked by open circles. They are assigned to adatoms A located on Ti atom rows. The gray circles represent adatoms B, which inclined towards the O atom rows in the images. The spots larger than the Cl adatoms, indicated by the arrows, are the TiO_x islands.

The height of adatoms A was 0.07 nm relative to the O-atom rows, as shown in the cross sections in Fig. 4(b). The relative height of an adatom is sensitive to the bias voltage, because the electrostatic force contributes to the tip-surface force. When the adatom accumulates or donates electrons, which is the case with Cl adatoms and Na adatoms, respectively, the adatom height relative to the uncovered surface is overestimated with a constant bias voltage. In the Kelvin probe force mode, the electrostatic force is canceled at each pixel of the topography. For example, the relative height of Na adatoms on TiO_2(110) was 0.17 nm, when a constant bias voltage, +0.2 V, was applied in imaging scans. In the Kelvin probe force mode, the relative height was reduced to 0.09 nm [9]. If we assume that the relative height of the Cl adatoms is reduced to a similar extent, the relative height in the Kelvin probe force topography should be 0.03 nm. With our signal-to-noise ratio, it may be difficult to recognize the small adatoms.

4. Conclusions

Chlorine adatoms on TiO_2(110) were observed with the STM, NC-AFM, and KPFM. Most adatoms were found on top of the Ti-atom rows of the surface. The local work function increased by 0.08 eV on the on-top Cl adatoms. Electron accumulation by the Cl adatom was hypothesized to cause a permanent dipole moment perpendicular to the surface. Charge transfer induced by individual halogen adatoms was first recognized with a Kelvin probe force microscope. Further

applications to catalyst models are promising.

References

[1] A. Kyomasu, T. Okuhara, and M. Misono: Chem. Lett. **19** (1990) 1643.

[2] G. J. Hutchings, F. King, I. P. Okoye, and C. H. Rochester: Catal. Lett. **23** (1994) 127.

[3] R. M. Lambert, R. L. Cropley, A. Husain, and M. S. Tikhov: Chem. Comm. (2003) 1184.

[4] D. I. Kondarides and X. E. Verykios: J. Catal. **174** (1998) 52.

[5] M. Nonnenmacher, M. P. O'Boyle, and H. K. Wickramasinghe: Appl. Phys. Lett. **58** (1991) 2921.

[6] *Noncontact Atomic Force Microscopy*, ed. S. Morita, R. Wiesendanger, and E. Meyer (Springer, Berlin, 2002).

[7] A. Sasahara, C. L. Pang, and H. Onishi: J. Phys. Chem. B **110** (2006) 13453.

[8] Y. Miyato, K. Kobayashi, K. Matsushige, and H. Yamada: Jpn. J. Appl. Phys. **44** (2005) 1633.

[9] A. Sasahara, H. Uetsuka, and H. Onishi: Jpn. J. Appl. Phys. **43** (2004) 4647.

[10] S. Kitamura, K. Suzuki, M. Iwatsuki, and C. B. Mooney: Appl. Surf. Sci. **157** (2000) 222.

[11] A. Sasahara, C. L. Pang, and H. Onishi: J. Phys. Chem. B **110** (2006) 17584.

[12] K. Hiehata, A. Sasahara, and H. Onishi: Nanotechnology **18** (2007) 084007.

[13] U. Diebold: Surf. Sci. Rep. **48** (2003) 53.

[14] D. Vogtenhuber, R. Podloucky, J. Redinger, E. L. D. Hebenstreit, W. Hebenstreit, and U. Diebold: Phys. Rev. B **65** (2002) 125411.

[15] E. L. D. Hebenstreit, W. Hebenstreit, H. Geisler, C. A. Ventrice Jr., D. A. Hite, P. T. Sprunger, and U. Diebold: Surf. Sci. **505** (2002) 336.

[16] U. Diebold, W. Hebenstreit, G. Leonardelli, M. Schmid, and P. Varga: Phys. Rev. Lett. **81** (1998) 405.

[17] D. Vogtenhuber, R. Podloucky, and J. Redinger: Surf. Sci. **454–456** (2000) 369.

[18] H. Onishi, K. Fukui, and Y. Iwasawa: Bull. Chem. Soc. Jpn. **68** (1995) 2447.

[19] A. Sasahara, S. Kitamura, H. Uetsuka, and H. Onishi: J. Phys. Chem. B **108** (2004) 15735.

[20] D. Ostermann, G. Walther, and K. D. Schierbaum: Phys. Rev. B **71** (2005) 235416.

[21] H. Onishi, T. Aruga, C. Egawa, and Y. Iwasawa: Surf. Sci. **199** (1988) 54.

[22] H. Onishi and Y. Iwasawa: Catal. Lett. **38** (1996) 89.

[23] K. Fukui, H. Onishi, and Y. Iwasawa: Phys. Rev. Lett. **79** (1997) 4202.

Figure captions

Figure 1. Model of TiO_2(110)-(1×1) surface.

Figure 2. (a) STM image of TiO_2(110)-(1×1) surface. Image size: 20×20 nm^2; sample bias voltage (V_s): +1.0 V; tunneling current (I_t): 1.0 nA. Cross sections obtained along the solid lines are presented. (b) STM image of TiO_2(110)-(1×1) surface exposed to Ar-diluted Cl_2 gas. Image size: 20×20 nm^2; V_s: +1.0 V; I_t: 1.0 nA. (c, d) Magnified images of areas indicated by squares in (a). (e) Cross sections along the dash-dott lines in (c) and (d).

Figure 3. (a) Topography and (b) work function maps of the Cl-adsorbed TiO_2 surface. Image size: 30×30 nm^2. Δf: -68 Hz. Peak-to-peak amplitude of the cantilever oscillation ($A_{p\text{-}p}$): 6.8 nm. Scanning speed: 3.3 ms/pixel. (c) Cross sections along the solid lines in the images. The triangles show the positions of the species along the cross sections. (d) The distribution of the work function shifts.

Figure 4. (a) The NC-AFM image of the Cl-adsorbed TiO_2 surface observed with a constant sample bias voltage, +1.4 V. Image size: 15×15 nm^2. Δf: -45 Hz. V_s: +1.4 V. $A_{p\text{-}p}$: 6.8 nm. (b) Cross sections obtained along the dash-dott lines in (a).

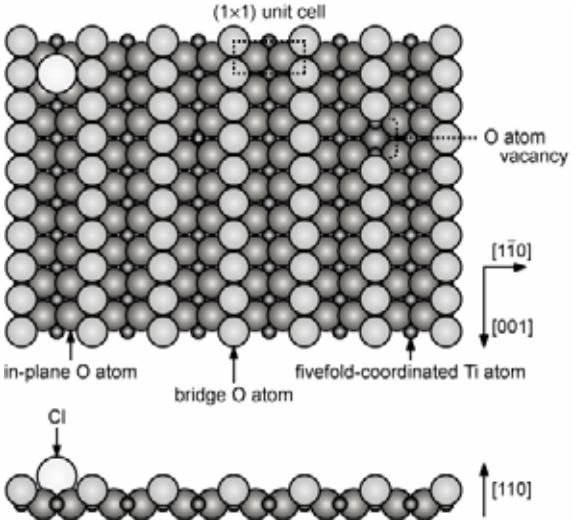

Hiehata et al. Figure. 1

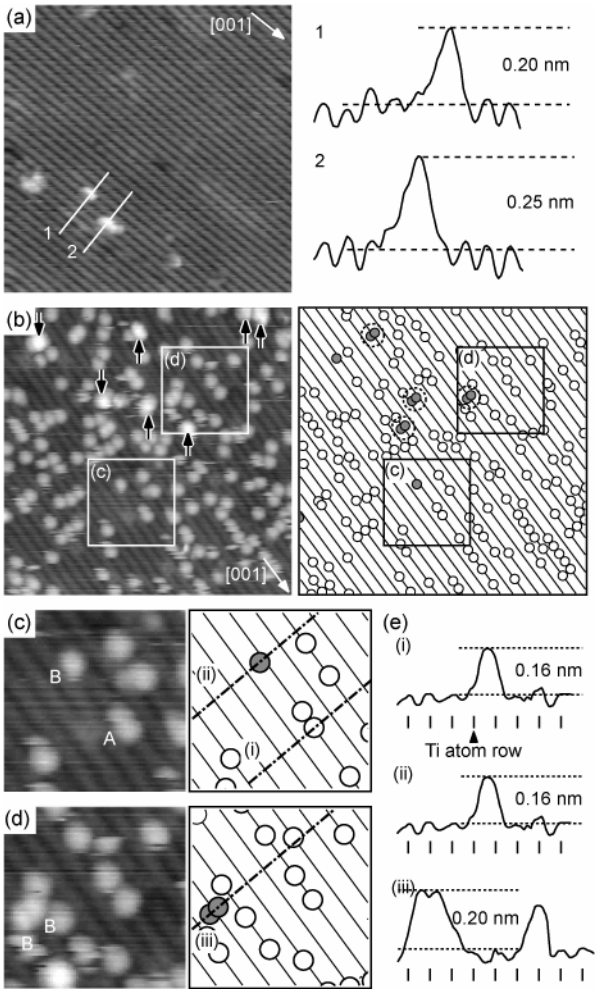

Hiehata et al. Figure 2

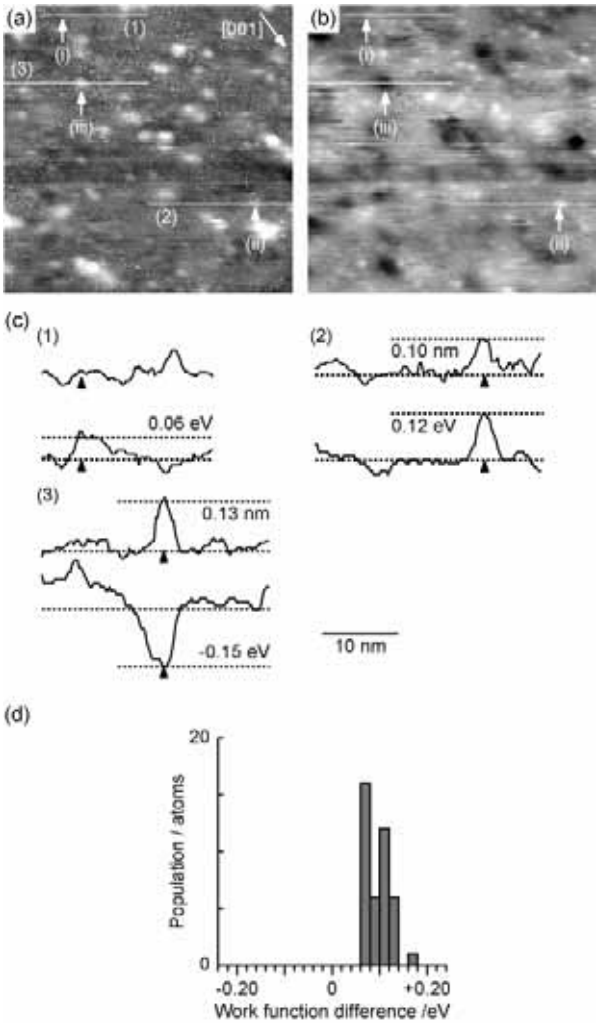

Hiehata et al. Figure 3

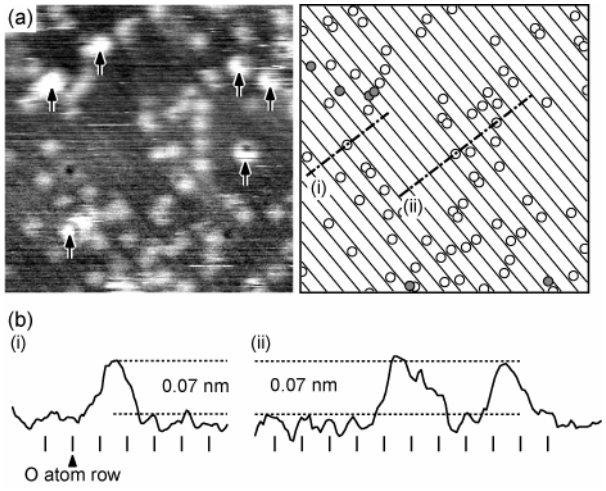

Hiehata et al. Figure 4